Eur. Phys. J. D **44**, 367–370 (2007)
DOI: 10.1140/epjd/e2007-00176-7

THE EUROPEAN PHYSICAL JOURNAL D

Planarity and stability of shock driven directly by the ninth laser beam from "Shenguang-II" laser facility

H. Shu[a], S.-Z. Fu, X.-G. Huang, M.-X. Ma, J. Wu, J.-J. Ye, J.-H. He, and Y. Gu

Shanghai Institute of Laser Plasma, P.O. Box 800-229, Shanghai 201800, P.R. China

Received 6 March 2007 / Received in final form 20 April 2007
Published online 1st June 2007 –

Abstract. Using the ninth laser beam (converted to 2ω) of "Shenguang-II" laser facility and the beam smoothing technology of lens-array [Appl. Opt. **25**, 377 (1986); Phys. Plasmas. **9**, 3201 (1995)], a shock wave with 700 μm (the root-mean-square of shock breakout time (RMS) RMS $\approx$ 6.32 ps) flat top was created. An Al-Al four-step target was designed to do research on shock wave stability in an Al target. And the shock stability experiment with the Al-Al four-step target indicated that the shock wave steadily propagated in the Al target of thickness of about 20–45 μm under the power density of $\sim 1.0 \times 10^{14}$ W/cm^2.

PACS. 51.30.+i Thermodynamic properties, equations of state – 91.60.Gf High-pressure behavior – 52.50.Lp Plasma production and heating by shock waves and compression

1 Introduction

Equation of state (EOS) data of matter in high pressure regime is a subject of interest for many fields of modern physics [1–12], including geophysics, astrophysics. In particular, in the inertial confinement fusion (ICF) [13–15] researches, compression efficiency and shock structure in fusion capsules critically depend on the EOS.

Some EOS exist for high pressure range come from numerical simulation and theoretical models [16]. Only a few experimental data are available to validate them. So far, high power lasers have been possible to drive Mbar shock waves in solid materials. But, in many laser driven shock wave experiments, the bad quality of shocks prevented them from being used as a quantitative tool in high pressure physics.

The planarity and stability [17,18] of the shock fronts are essential to obtain accurate EOS data. This requires to choice the target thickness properly. In case of a very thin target, the shock breakout time is earlier than the laser pulse peak time, leading to an instable shock front (still in acceleration phase). On the other hand, rarefaction wave from the laser illumination side can interact in case the target is too thick.

In this paper, a shock wave with 700 μm (the RMS of shock breakout time $\delta t \approx 6.32$ ps) flat top was created using the ninth laser beam (converted to 2ω) of "Shenguang-II" laser facility and the beam smoothing technology of lens-array. An Al-Al four-step target was designed to do research on shock wave stability in an Al target. And the shock stability experiment with the Al-Al four-step target indicated that the shock wave steadily propagated in the Al target of thickness of about 20–45 μm under the power density of $\sim 1.0 \times 10^{14}$ W/cm^2.

[a] e-mail: shuhua_79@hotmail.com

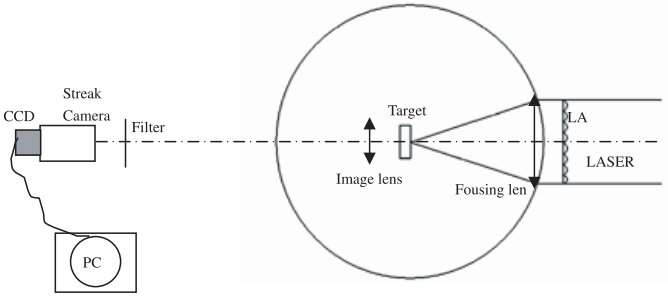

Fig. 1. Experimental set-up.

2 Experimental set-up

The experiment was performed using the "Shenguang-II" Nd: Glass laser (converted at $\lambda = 0.527$ μm) of the National Laboratory on High Power Laser and Physics. The temporal profile of the laser was a square with a rise time of 300 ps give a full width at half maximum (FWHM) of 2 ns. In order to eliminate the large scale spatial modulation and to obtain a flat-top profile in the focal spot, we used lens-array [19,20]. Characteristics of our optical system (Lens + LA) were such that our focal spot had a $\sim$1 mm diameter flat region. The absorbed laser intensity in the focal spot was $\sim 10^{14}$ W/cm^2. The experimental set-up is shown in Figure 1.

Fig. 2. Schematic of Al-Al four-step target.

The principal diagnostic was a streak camera which allowed us to determine the shock breakout time from the target rear side. Shock breakout signals are collected by an chromatic system and imaged on the slit of the streak camera with an 11× magnification (this magnification is well matched to our receiving system), giving spatial resolution ∼10 μm and time resolution ∼12 ps.

3 Target

3.1 Target fabrication

The targets used in the experiments were made-up of a series of thin foils with varied thicknesses with thickness uniformity <0.5% d (d is the thickness of the foil) and surface roughness R_q < 50 nm (R_q is the root mean square (RMS) roughness of the target surface). There are three steps in the target manufacturing process: (1) let the thin foil flatten in a glass base plate then, the foils were measured and the satisfactory foils were picked out; (2) various shapes of targets (such as Al-Al four-step target, show in Fig. 2) were fabricated on the glass base plate using the picked foils; (3) assemble the targets namely, the formed targets were transferred from the glass base to the target shelf. An Al-Al four-step target was designed to do research on shock wave stability in an Al target. The sketch map of the Al-Al four-step target is shown in Figure 2. The Al-Al four-step targets are made up of thin foils with various thicknesses.

3.2 Targets measurement

A white-light interferometer was used, with a theoretical precision of 1 Å for surface measurement. Each target was scanned several times during the fabrication process, and the interferometer was recalibrated against height standards every three hours. There are three steps in the target measurement process: (1) it is the thickness-measurement of single foil when it is on the glass base plate; (2) after several foils were combined together (see Fig. 2) and the thicknesses of the steps of the target were measured again; (3) it is the thickness-measurement of the targets when they were transferred to the target shelf. A flag was labeled on the target so that the white-light interferometer scanned the same place. The target will be thrown away if the three measurement results do not match. The measurement profile of Al-Al four-step target is shown in Figure 3.

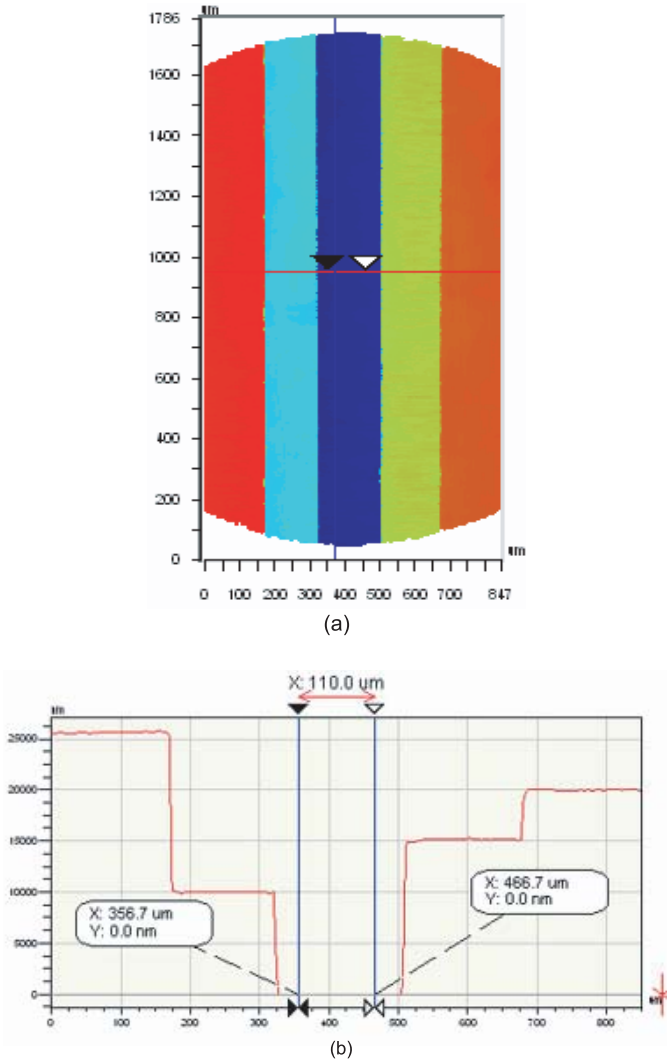

Fig. 3. (Color online) (a) Two-dimension profile and (b) one-dimension profile of Al-Al four-step target.

4 Experimental results

4.1 Flat target experiment

In order to obtain a plane shock wave, the beam smoothing technology of lens-array [19,20] was used. The lens-array was composed of array of nearly 100 similar lenses (see Fig. 1). This combination focus system makes the driving laser intensity uniformly distributed in space on the target. The lens-array was located in front of a principal lens (see Fig. 1). The lens-array approach is similar to the phase zone plates [21,22] (PZP) approach except that the PZP alternately introducing a 0 or π phase difference on the incident beam. We will describe result obtained with direct drive with lens-array.

The primary diagnostic was a streak camera. The streak camera's slit was orthogonal to the target and acted to check shock breakout uniformity over the plane target. The root-mean-square deviation (RMS) of shock breakout time on varied space was used as an evaluation criterion

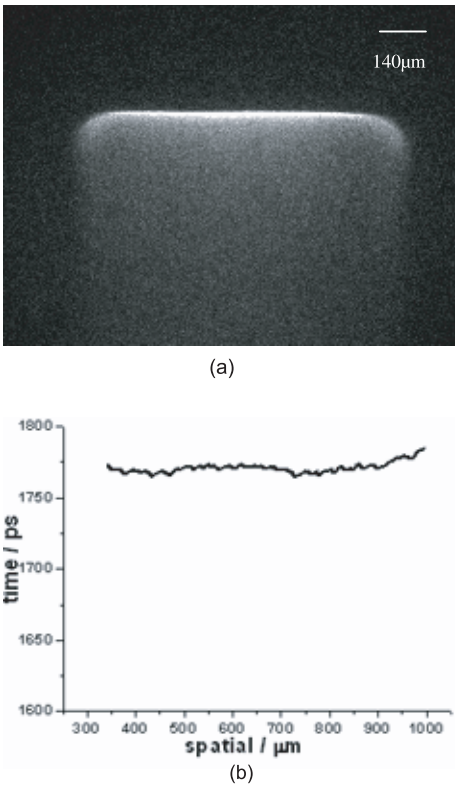

Fig. 4. (a) Streak image of Al flat target. (b) Plot of relative shock breakout time vs. spatial position.

of shock wave flatness. A streak image of the Al flat target with 30 μm thickness is shown in Figure 4a. A plot of the relative shock breakout time vs. spatial position (distance along camera slit) is shown in Figure 4b. The total region of the shock wave was estimated as 900 μm (FWHM). The central flat region of shock wave was about 700 μm diameter, with a variation in breakout time RMS = 6.32 ps.

4.2 Shock wave stability

4.2.1 Simulation

The question of shock wave stationarity is influenced both by the fact that the relaxation wave, originating on the target front, reaches the shock wave [17], and by the fact that, even for a constant laser irradiation, the generated pressure tends to decrease [23]. A proper radiation hydrodynamic simulation serves as an important tool in predicting proper target thickness that can avoid the effects of preheating and also ensure steady state shock wave propagation conditions. The Al target has been studied in detail using a one-dimensional and three-temperature hydrodynamic code JB [24]. The JB code is a one-dimensional and three-temperature hydrodynamic code coupling with superthermal electron transportation and a self-consistent electric field. The main physical processes considered in the code include inverse bremsstrahlung and anomalous laser absorption, coulomb interaction of electron-ion, free-

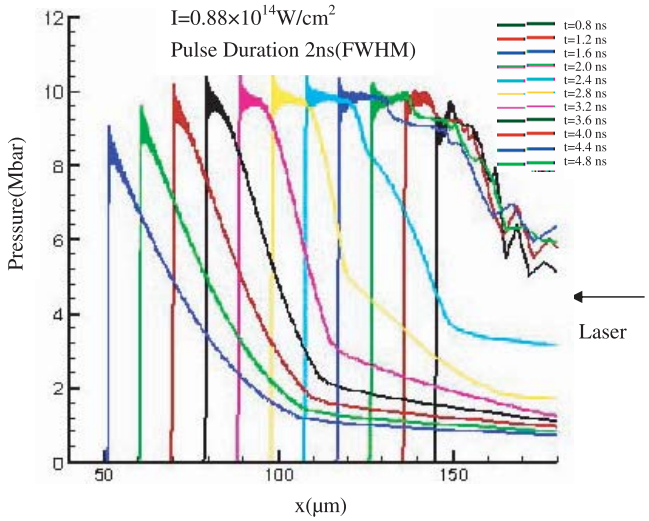

Fig. 5. (Color online) Simulated time and space resolved shock pressure profile in Al target.

free, and free-bond processes of electron photon, the average atomic model and local thermodynamic equilibrium in the ionization process, free-free, free-bond, and bond-bond processes for photon's opacity, coulomb collisions between superthermal electrons and thermal ions for the scattering mean-free-path, the theoretic equation of state given by the Thomas-Fermi model, and experimental data from the high explosive loading facility in the respective ranges of ultrahigh and low pressures, etc.

The simulation was performed for a single layer of Al target (2.7 g/cm^3) for absorbed laser irradiation of and 0.88×10^{14} W/cm^2 ($\lambda = 0.527$ μm, pulse duration (FWHM) = 2.0 ns). As shown in Figure 5, the pulse shape of the driven laser used in the simulation has a square profile with a rise and fall time of 300 ps. Figure 5 shows the simulated time and space resolved shock pressure profile. The simulations show that the duration of shock wave stable propagation time is about 4.0 ns (the shock stable propagation distance is about 94 μm). This agrees well with the criteria report in previous paper [25].

4.2.2 Experiment

An Al-Al four-step target was designed to do research on shock wave stability in an Al target. It is hard to add much more steps(more than four steps) in the limited plane region ($\sim$700 μm), so the thicknesses of the steps of the target were selected in the range which we were interested in. Shock breakout signal obtained with Al-Al four-step target was shown in Figure 6a. Plot of step thicknesses vs. shock transit times is shown in Figure 6b. Table 1 shows the step thicknesses, shock transit times and shock velocity (the Al base is 20 μm).

The blue line and the red line in Figure 6b represent linear fitting of first three data and first four data respectively. Two fitted lines are in close agreement. This indicate that the shock wave steadily propagated in the Al

Table 1. Measured step thicknesses and shock transit times for Al-Al four-step target.

Step thickness (μm)	9.96 ± 0.081	15.25 ± 0.12	20.08 ± 0.17	25.63 ± 0.21
Transit time (ps)	470 ± 8.1	730 ± 8.1	960 ± 8.3	1230 ± 8.1
Shock vel. (μm/ns)	21.19 ± 0.4	20.89 ± 0.3	20.92 ± 0.25	20.84 ± 0.2

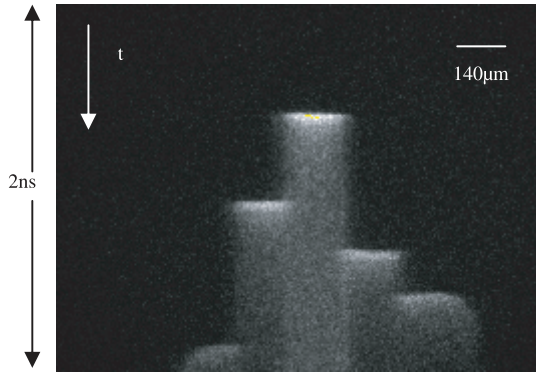

(a)

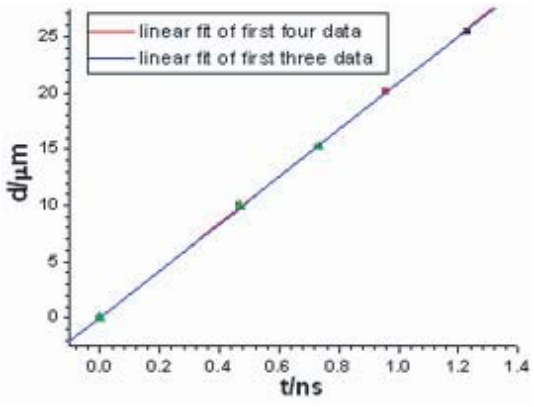

(b)

Fig. 6. (a) Streaked image of Al-Al four-step target. (b) Measured step thicknesses vs. shock transit times.

target of thickness of about 20–45 μm. The experiment result was consistent with the numerical simulation.

5 Conclusion

Using the ninth laser beam (converted to 2ω) of "Shenguang-II" laser facility and the beam smoothing technology of lens-array, a shock wave with 700 μm (the RMS of shock breakout time $\delta t \approx 6.32$ ps) flat top was created. The flat target experiment shows that the application of beam smoothing technology of lens-array in equation of state is very successful. And the shock stability experiment with the Al-Al four-step target indicated that the shock wave steadily propagated in the Al target of thickness of about 20–45 μm under the power density of $\sim 1.0 \times 10^{14}$ W/cm^2.

The authors gratefully acknowledge the valuable support for the experiments by the "Shenguang-II" technical crews, and especially to Luo Pinqin for providing the simulation results.

References

1. C.G.M. van Kesse, R. Sigel, Phys. Rev. Lett. **33**, 1020 (1974)
2. F. Cottet et al., Phys. Rev. Lett. **52**, 1884 (1985)
3. A. Ng, D. Parfeniuk, L. DaSilva, Phys. Rev. Lett. **54**, 2604 (1985)
4. R.G. McQueen, S.P. Marsh, J. Appl. Phys. **33**, 654 (1962)
5. L.B. Da Silva et al., Phys. Rev. Lett. **78**, 483 (1997)
6. M. Koenig et al., Phys. Rev. Lett. **74**, 2260 (1995)
7. D. Batani et al., Phys. Rev. B **61**, 9287 (2000)
8. A. Benuzzi et al., Phys. Rev. E **54**, 2162 (1996)
9. D. Batani et al., Phys. Rev. Lett. **88**, 235502 (2002)
10. D. Batani et al., Phys. Rev. Lett. **92**, 065503 (2004)
11. A.M. Evans et al., Laser. Part. Beams **14**, 113 (1996)
12. G.W. Collins et al., Science **281**, 1178 (1998)
13. S.W. Hann et al., Phys. Plasmas **2**, 2480 (1995)
14. J.D. Lindl, Phys. Plasmas **2**, 3933 (1995)
15. T.R. Dittrich et al., Phys. Plasmas **6**, 2164 (1999)
16. R.M. More, K.H. Warren, D.A. Young, G.B. Zimmerman, Phys. Fluids **31**, 3059 (1988)
17. D. Batani et al., Eur. Phys. J. D **23**, 99 (2003)
18. T. Löwer et al., Phys. Rev. Lett. **72**, 3186 (1994)
19. X.M. Deng, X.C. Liang, Z. Chen, Appl. Opt. **25**, 377 (1986)
20. S.Z. Fu et al., Phys. Plasmas. **9**, 3201 (1995)
21. M. Koenig et al., Phys. Rev. E **50**, R3314 (1994)
22. D. Batani et al., Eur. Phys. J. D **19**, 231 (2002)
23. P. Mora, Phys. Plasmas. **25**, 1051 (1982)
24. L. Dongxian et al., in *Proceedings of the International Conference on Computational Physics, Beijing, 1988,* edited by L. Denyuan, D. Feng (World Scientific, Singapore, 1989), p. 156
25. G. Yuan et al., Laser Part. Beams **14**, 157 (1996)